Vacuum 141 (2017) 139–143

Contents lists available at ScienceDirect

Vacuum

journal homepage: www.elsevier.com/locate/vacuum

The effect of AlGaN bulk and AlGaN/GaN superlattice cladding layers on performance characteristics of deep violet InGaN DQW lasers

Maryam Amirhoseiny [a], Ghasem Alahyarizadeh [b], *

[a] Buein Zahra Technical University, Buein Zahra, Qazvin, Iran
[b] Engineering Department, Shahid Beheshti University, G.C., P.O. Box 1983969411, Tehran, Iran

ARTICLE INFO

Article history:
Received 2 December 2016
Received in revised form
12 February 2017
Accepted 3 April 2017
Available online 5 April 2017

Keywords:
InGaN quantum well laser
Superlattice
Cladding layers
Optical properties
Numerical simulation

ABSTRACT

This paper reports performance characteristics of InGaN-based DQW laser diodes with different SLS cladding layer (CL) structures using the ISE TCAD software. LDs with SLSs as CLs were shown to have superior optical and electrical properties compared to LDs with bulk AlGaN CLs.The simulation results show the variation of output power, threshold current, slope efficiency, and differential quantum efficiency (DQE) from 13.51 to 10.88 mA, 20.92 to 41.27 mW, 1.83 to 1.87 W/A and 57.88 to 59.10%, for bulk to SLS CLs. Results show the increased operating current, electron and hole carrier densities and radiative recombination which enhanced output power and reduced threshold current for the structure with the SLS down CL. Using SLS in upper CL doesn't have significant effect on operating current, it increase the slope efficiency and DQE. Using SLS structure simultaneously in up and down CLs enhances the output power, DQE and slop efficiency, and decreases the threshold current.

One of the most important issues related to III-nitride devices is difficultly to grow the thick AlGaN cladding layer required for optical confinement, due to the formation of cracks during growth. These cracks are due to the stress introduced in the AlGaN cladding layers caused by lattice mismatch, and the difference in thermal expansion coefficients between the AlGaN cladding layer and GaN layers. This problem can be solved with using superlattice structures in the cladding. There are several experimental research reports that have used SLS structure to overcome the above mentioned problems and increased device efficiency. However, the physics and theory of SLS structure effects haven't discussed comprehensively [1–6]. The main advantage of utilizing the superlattices cladding layers are firstly, decreasing the lattice mismatch stresses during growth. AlGaN/GaN strained layer superlattices (SLSs) have been employed for strain relief of the cladding layer. Secondly, mg-doped AlGaN/GaN superlattices have also shown an enhanced hole concentration. A required valence band edge oscillation is provided by using superlattice cladding layers which involved various alloys with different valence band edge positions. This technique which was proposed by Schubert et al. [10] increases the total hole concentration. The deep acceptors were allowed to flow in the barriers to ionize into the valence band of provided neighboring narrow band-gap material. On the other hand, the large polarization fields are in the nitride materials [11]. applying AlGaN/GaN superlattice will significantly reduce polarization fields which are due both to the piezoelectric and spontaneous effects in and between the strain AlGaN layers [12]. The reduced polarization filed caused by valence band oscillation results in further enhancement of the hole concentration. The mechanism for enhancement of hole concentrations is based on the periodic oscillation of the valence-band edge which was explained by Kozodoy et al. [7]. Applying a periodic oscillation of the valence energy band edge provides an appropriate condition to overcome low doping efficiency of deep acceptor layers. When the energy band edge is extreme below the Fermi energy level, acceptors are ionized that results in higher holes accumulation in the band edge close to the Fermi levels. Although SLS layers cause to that the free carriers are separated into parallel sheets, higher averaged carrier densities than those in a simple bulk layer will be provided. The impact of the AlGaN/GaN superlattices on the average carrier density is addressed in this work through the numerical simulation. To the best of our knowledge there is no comprehensive numerical study on the theoretical concept of strained-layer-superlattice cladding layer structures on InGaN laser diodes.

In this work the effect of different structure of AlGaN/GaN superlattice cladding layers on InGaN double-quantum-well

* Corresponding author.
E-mail address: g_alahyarizadeh@yahoo.com (G. Alahyarizadeh).

http://dx.doi.org/10.1016/j.vacuum.2017.04.002
0042-207X/

(DQW) laser diode performance has been investigated. The structure designs consisted of four structures which their cladding layers are bulk layers, down SLS layer (SLSd), up SLS layer (SLSu), and two side SLS layers (SLST).

The schematic of the main laser structure under study are shown in Fig. 1(a). The basic structures extracted and modified from the real laser structure fabricated by Nakamura [8]. The structure of laser consists of a 0.4 μm n-GaN, a 0.1 μmn-$In_{0.05}Ga_{0.95}N$ compliance layer, a0.42 μm n-$Al_{0.07}Ga_{0.93}N$ cladding layer and a 0.1 μm n-GaN waveguiding layer. The double quantum well active region consists of two 2.5 nm $In_{0.082}Ga_{0.918}N$ wells that are sandwiched between 8.5 nm of GaN barriers. A 15 nm p-$Al_{0.22}Ga_{078}N$ EBL is used to reduce electron leakage on the top of the active region. Next layers consist of a 0.1 μm p-GaN waveguiding layer, a0.42 μm p-$Al_{0.07}Ga_{0.93}N$ cladding layer and a 0. 1 μm p-GaN layer, respectively. The doping concentrations of n-type and p-type layers are1×10^{18} and $5.5 \times 10^{18} cm^{-3}$, respectively. The laser area is 1 μm * 300 μm. The reflectivity of the back and front mirrors is considered equal to 50%. Each SLS cladding layer consists of 84 pair 2.5/2.5 nm $Al_{0.08}Ga_{0.92}N$/GaN layers.

Several equations such as the Poisson equation, the Schrodinger equation, the photon rate equation, the current continuity equations and the scalar wave equation was solved in the laser simulation process using a two dimensional ISE TCAD simulator. The physical parameters of the ternary and quaternary alloys which are used in the simulation are interpolated by the binary alloys that can be expressed by the equations mentioned before [11–13].

Fig. 1(b) shows the electrostatic potential, energy bandgap, conduction band and the valence band profile of InGaN DQWs structure with SLST layers. Zero of the horizontal axis in this figure is the first edge of p-contact layer and the figure is shown a part of structure including p-cladding to n-cladding layers. It can be seen that the superlattice structures produce the required valence band edge oscillation by employing alloys with different valence band edge positions. This technique increases the overall hole carrier concentration. The deep acceptors were allowed to flow in the barriers to ionize into the valence band of provided neighboring narrow band-gap material, rather than into the deeper valence band of the host material [4]. If the quantization and polarization effects are neglected and the valence band–edge modulation is provided only by the discontinuity ΔE_V, then holes will accumulate at each interface, so a dense array of interfaces will maximize the spatially averaged carrier density. The polarization field significantly increases the band bending resulting in a higher hole concentration.

The optical intensity of the deep violet InGaN laser diodes with bulk and different SLS cladding layers structures are shown in Fig. 2(a). The laser diode with SLS cladding on both side, top and down part has a highest optical intensity value of 7.5×10^{14} compared to 2.5×10^{14} for laser diode with bulk cladding layers due to the enhancement in the optical confinement, current densities, and radiative recombination. Optical intensity peak position depends on the radiative recombination rate and carrier density in the quantum wells. By using SLS cladding layer, the carrier density and thus radiative recombination are changed in QW from QW_1 to QW_2. Therefore the peak position and optical intensity shape are not the same in different structures.

Fig. 2(b) show electron current densities in QWs of deep violet $In_{0.082}Ga_{0.918}N$/GaN DQW LDs with different cladding layer structures. As shown in Fig. 2(b), the LDs with SLSd and SLST have the higher QW electron and hole current densities in the active region, which means that these structures provides the highest electron confinement. An AlGaN/GaN superlattice will reduce polarization fields which are due both to the piezoelectric and spontaneous effects in and between the strain AlGaN and GaN layers [6]. The reduced polarization fields induce the valence band oscillation which created by the valence band discontinuity, result in further enhancement of the hole carrier concentration.

Fig. 3(a) shows the threshold current, slope efficiency, output power and DQE of the deep violet InGaN DQW lasers with different cladding layer structures. The reduction in the threshold current can be seen from Bulk to SLST cladding layer structure. Based on Fig. 2(b), it can been that superlattice structure in the down cladding layers which there are in the SLSd and SLST increase the electron and hole current densities. Consequently, the increase in electron and hole current concentration leads to a reduction in the vertical resistance for the SLSd layer, which resulted in the enhancement of carriers radiative recombination and output power, as seen in Figs. 3 and 4. In addition, holes flow is smoother in the SLSu structure which increased carrier recombination and decreased the electron overflow (Fig. 2(b)). Although, SLSu has lower output power due to the lower operating current compare to SLSd, but it has higher slop efficiency and DQE which is clear in Fig. 3(a). Therefore using the SLS structure simultaneously in up

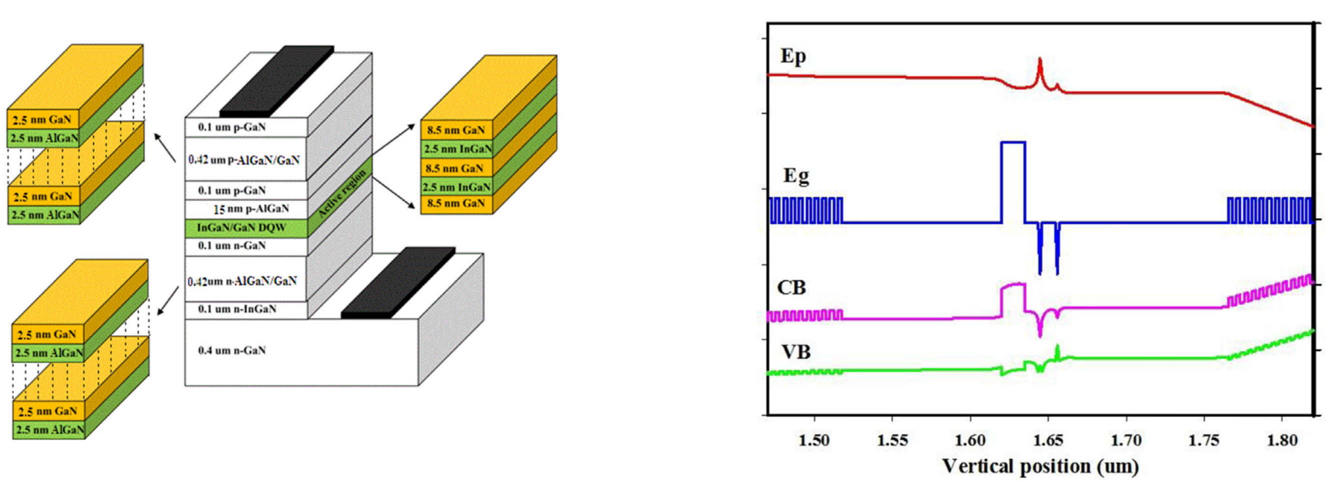

(a) (b)

Fig. 1. (a) Schematic diagram of laser structures, (b) the electrostatic potential, energy bandgap, conduction band and the valence band profile of SLSTInGaN DQWs lasers.